Accident Analysis and Prevention 154 (2021) 106055

Contents lists available at ScienceDirect

Accident Analysis and Prevention

journal homepage: www.elsevier.com/locate/aap

Steering or braking avoidance response in SHRP2 rear-end crashes and near-crashes: A decision tree approach

Abhijit Sarkar [a,*], Jeffrey S. Hickman [a], Anthony D. McDonald [b,c], Wenyan Huang [d], Tobias Vogelpohl [e], Gustav Markkula [f]

[a] Virginia Tech Transportation Institute, United States
[b] Texas A&M University, United States
[c] Texas A&M Transportation Institute, United States
[d] Virginia Polytechnic Institute and State University, United States
[e] Technische Universität Braunschweig, Germany
[f] University of Leeds, United Kingdom

ARTICLE INFO

Keywords:
Avoidance response
Gaze eccentricity
SHRP 2 naturalistic driving
Random forest
Driver maneuver
Rear-end events

ABSTRACT

Objective: The paper presents a systematic analysis of drivers' crash avoidance response during crashes and near-crashes and developed a machine learning-based predictive model that can determine driver maneuver using pre-incident driver behavior and driving context.

Methods: We analyzed 286 naturalistic rear-end crashes and near-crashes from the SHRP2 naturalistic driving study. All the events were manually reduced using face video (face and forward) and kinematic responses. In this paper, we developed new reduction variables that enhanced the understanding of drivers' gaze behavior and roadway attention behavior during these events. These features reflected how the event criticality, measured using time to collision, related to drivers' pre-incident behavior (secondary behavior, gaze behavior), and drivers' perception of the event (physical reaction and maneuver). The imperative understanding of such relations was validated using a random forest- (RF) based classifier, which efficiently predicted if a driver was going to brake or change the lane as an avoidance maneuver.

Results: The RF presented in this paper effectively explored the nonlinear patterns in the data and was highly accurate (~96 %) in its prediction. A further analysis of the RF model showed that six features played a pivotal role in the decision logic. These included the drivers' last glance duration before the event, last glance eccentricity, duration of 'eyes on road' immediately before the event, the time instance and criticality when the driver perceives the threat as well as acknowledge the threat, and possibility of an escape path in the adjacent lane. Using partial dependency plots, we also showed how different thresholds of these feature variables determined the drivers' maneuver intention.

Conclusions: In this paper we analyzed driving context, drivers' behavior, event criticality, and drivers' response in a unified structure to predict their avoidance response. To the best of our knowledge, this is the first such effort where large-scale naturalistic data (crashes and near crashes) was analyzed for prediction of drivers' maneuver and determined key behavioral and contextual factors that contribute to this avoidance maneuver.

1. Introduction

In 2015 (National Highway Traffic Safety Administration, 2017), rear-end crashes were the most prevalent crash type involving another vehicle that resulted in an injury or property-damage only (32.4 % and 33.9 %, respectively), and the third most prevalent crash type in fatal crashes involving another vehicle (6.8 %). Most of these crashes occur when the following vehicle (or striking vehicle) makes contact with a stopped or decelerating lead vehicle (Najm et al., 2013). Naturalistic driving studies and national crash databases have found that inattention (likely visual in nature) appears to play a significant role in rear-end crashes (Eiríksdóttir, 2016; Engström et al., 2013; Harb et al., 2009; Klauer et al., 2006; Victor et al., 2015). Automated driving systems (ADS) have the potential to significantly reduce these rear-end crashes

* Corresponding author at: Virginia Tech Transportation Institute, 3500 Transportation Research Plaza, Blacksburg, VA, 24061, United States.
E-mail address: asarkar@vtti.vt.edu (A. Sarkar).

https://doi.org/10.1016/j.aap.2021.106055
Received 16 April 2020; Received in revised form 28 December 2020; Accepted 19 February 2021
Available online 7 March 2021
0001-4575/

(National Transportation Safety Board; Najm et al., 2013). However, their success depends on the extent to which they are designed within human capabilities (Lee, 2018; Seppelt and Victor, 2016). In rear-end crashes, the driver's avoidance response decision (e.g., steering and/or braking) is a critical aspect of the safety of the response. Understanding the factors that influence this decision may lead to more accurate process models of driver behavior in rear-end collisions. Such models can be used to predict driver responses to estimate the safety benefits of ADS and in turn design effective warnings for driver responses and take-over requests (Bärgman et al., 2017; Markkula et al., 2018; McDonald et al., 2019a, b).

Different approaches have been used to assess drivers' choice of avoidance response in crash/near-crash situations. Kaplan and Prato (2012) used data from a national crash database (General Estimates System or GES) to evaluate attributes that predicted drivers' attempted crash avoidance maneuvers. Although the authors did not report findings for rear-end crashes, they reported that 68 % of the crashes involved no avoidance response, followed by braking, steering, braking and steering, and other maneuvers. Harb et al. (2009) also used GES data, but only reported the drivers' avoidance response as a binary variable (yes/no). However, they stratified their results by three different crash types: rear-end, head-on, and angle crashes. The three most important variables in classifying if a driver made an avoidance maneuver in a rear-end crash (compared to no avoidance maneuver) were physical impairment (fatigue and/or alcohol), distraction, and speed limit. Although these data are informative, they have several limitations. The accuracy of data from post-crash reconstruction relies heavy on witness testimony and/or a clear indication of vehicle kinematics (such as skid marks). The authors noted this as a limitation and reported that over 60 % of drivers' avoidance responses were coded as "unknown". This suggests there was insufficient data to determine the avoidance response made by the driver, or even if an avoidance response was made at all. In fact, the 68 % estimate of lacking avoidance response cited above (Kaplan and Prato, 2012) is strongly at odds with naturalistic crash data which have shown that the majority of crashes include braking and/or steering avoidance responses (e.g., Engström et al., 2013). Moreover, these data do not include measures of drivers' visual attention to the forward roadway prior to the crash, which is important in determining drivers' avoidance response (Markkula et al., 2016; Svärd et al., 2017; Venkatraman et al., 2016; Xue et al., 2018).

Simulator studies using a car-following or vehicle cut-in paradigm have also been used to evaluate driver's avoidance response in rear-end crash scenarios. Hu et al. (2017) used a cut-in scenario to evaluate drivers' decision to brake or steer (i.e., change lanes). Driver factors, such as personality traits, and the driver's perceived safe zone largely predicted the avoidance response during the vehicle cut-in. The authors found that age and drivers' geographic location (or location of the data collection site) affected a braking or steering response in a simulated car following paradigm. Venkatraman et al. (2016) reported that perceptual variables, such as optical angle and tau, were better predictors of drivers' decision to brake or steer than alerts from a collision warning system in a simulated car following paradigm. Braking was more likely as the driver got closer to the lead vehicle, and, in turn, less likely to steer. Xue et al. (2018) found that an evidence accumulation model (i.e., multiple sources of evidence per time unit), which included brake lights, was better at predicting brake response time than a looming threshold model (i.e., optical expansion). Although these simulator studies are informative, they were performed in a controlled environment where the drivers' eyes were always on the road and considered a small number of independent variables. The simulator is unable to account for the complexities of natural driver behavior, as many factors are likely to influence drivers' decision to perform an avoidance maneuver.

Several studies have investigated naturalistic driving data for predicting driver responses. Dozza (2013) used naturalistic driving car and truck data to assess driver response times for evasive maneuvers in crashes and near-crashes (not limited to rear-end events). Not surprisingly, Dozza (2013) found that attendance to eyes-off-road and secondary tasks delayed response times. Markkula et al. (2016) assessed naturalistic driving behavior in a sample of rear-end crashes and near-crashes. This included events with/without visual distraction. Braking response times were more strongly dependent on visual looming than brake light onset. The authors used an accumulation model to predict drivers' response to a takeover request from an ADS in a rear-end crash scenario. Braking was hypothesized to function much like that presented by Dozza (2013); however, steering was dependent on early detection of the threat or awareness that braking alone would not mitigate/prevent the threat (both modulated by looming and knowledge that steering to another lane is available).

The prior studies have identified eyes-off-road distractions, driver impairment, speed limits, driver personality factors, and accumulated optical evidence as critical factors in a driver's decision to steer or brake in response to a rear-end emergency. However, these studies did not include the driver's gaze eccentricity, which has been shown to adversely impact lane keeping and braking response to a lead vehicle (Lamble et al., 1999; Senders et al., 1967). In addition, prior work (Hu et al., 2017) established that tree-based machine learning approaches, such as decision trees and random forests, are effective methods for inference in rear-end emergencies. The prior work is limited in analyses of naturalistic driving data and in its focus on broad gaze metrics (e.g., eyes-on-road/eyes-off-road) rather than specific measures of gaze eccentricity. Thus, our two main research questions for this analysis constitute clear advances beyond the prior work: (1) What factors determine whether drivers will brake and/or steer to avoid a real-world rear-end crash/near crash?; and (2) How do these driver responses depend on gaze eccentricity? We address these questions with a machine learning analysis of drivers' avoidance response choices during rear-end crashes and near-crashes in the SHRP 2 s Strategic Highway Research Program (SHRP 2) dataset. We analyzed a large set of rear-end events in the SHRP 2 data set, extracting from each event a range of new information relevant to our research questions (Section 2). Then, we used this extracted event-level information as training data for a random forest classifier, predicting driver maneuver in each event (Section 3). Finally, we used this model for an inferential analysis of the factors that influence braking/steering decisions (Section 4 and Section 5).

2. Methods

Data from rear-end car crashes and near-crashes from the second

Table 1
A step by step process of data post processing for feature generation and aggregation.

Step 1	Access all NDS event data and existing reduction data for SHRP2 data
Step 2	Select events with: 1 Rear end crashes/near-crashes with subject driver at fault 2 Maximum speed >15 m/s 3 All kinematic data available (speed, acceleration, radar, gyro etc.)
Step 3	Perform additional video review and annotation development pertaining to driver decision (see Section 2.1.2)
Step 4	Compute new feature variables (Section 2.2–2.5)
Step 5	Combine new feature variables (Steps 3 and 4) with existing reduction variable (Step 2)

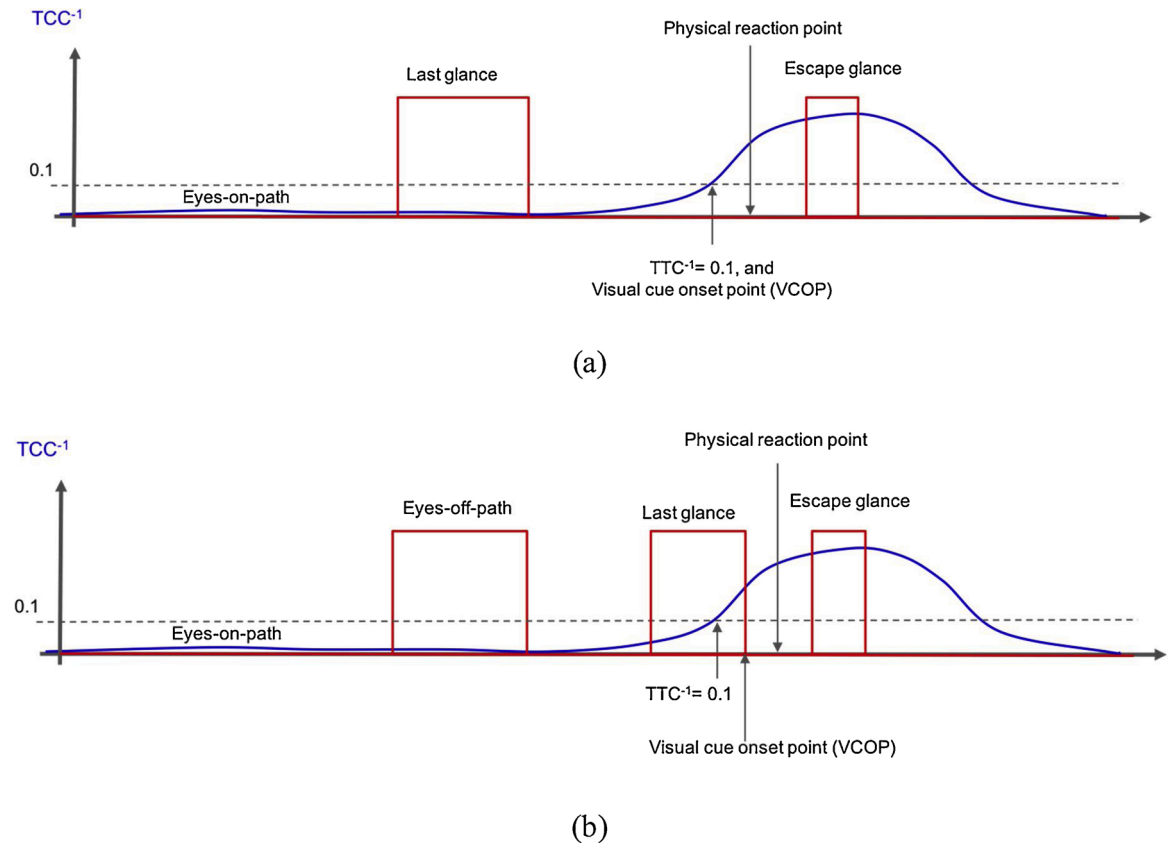

Fig. 1. Schematic depiction of two VCOP cases: (a) eyes-on-threat (b) eyes-off-threat. In both cases the $\boldsymbol{TTC}^{-1}$ threshold was 0.1.

Strategic Highway Research Program Naturalistic Driving Study (SHRP2 NDS) were used in this study. A detailed overview of the SHRP2 NDS methodology can be found in Dingus et al. (2015). SHRP2 NDS collected two petabytes of data from over 3000 participants, encompassing nearly 40 million miles of naturalistic driving data. The InSight website (https://insight.shrp2nds.us/) has more information about the study and detailed descriptions of available variables. Post processing of SHRP2 NDS data identified and analyzed 41,476 events using the event analysis protocol, including all crashes, near crashes, and some baseline events. Of these, 391 rear-end crash and near-crash events where the subject vehicle was the following vehicle were used in this analysis. All the rear-end events included at least two light vehicles (excluding rear-end events with a pedestrian, pedalcyclist, heavy truck, etc.). After initial review, thirty-six of these events were removed due to one or more of the following: (1) maximum speed less than 15 m/s, (2) no valid data for speed, acceleration, or gyroscope data, (3) no radar data point from the lead vehicle. The existing data annotations from the 355 rear-end subject vehicle striking events in SHRP2 NDS were reviewed. Based on the review process, we developed several new reduction variables. These variables were merged with the existing annotations in SHRP2 NDS. Table 1 shows a step-by-step process on how this was executed.

2.1. Data reduction

2.1.1. Existing data reduction and radar data pulled from SHRP 2

The existing annotations (see https://insight.shrp2nds.us/ for complete list of variables) and radar data from the 355 rear-end crashes and near crashes were extracted from the SHRP2 NDS data repository. This included one minute of radar data and subject driver eye glance behavior (i.e., where the subject driver was looking, categorical data with 19 levels, such as 'Forward', 'Transition', 'Rearview Mirror', etc.). In addition, existing categorical and continuous variables from this prior data reduction were included including, (i) time stamp for the selected event, (ii) subject driver variables (gender, age), (iii) time stamp of the evasive braking and/or steering response by the subject vehicle, (iv) time stamp for start of subject physical reaction (i.e., subject driver's physical reaction to awareness of impending crash or near crash), (v) driver glance data, (vi) driver impairment, and (vii) secondary tasks.

2.1.2. New data reduction

The videos from the 355 rear-end events were manually reviewed to support the specific research questions mentioned in the Introduction, extracting an extended set of variables, as defined in Table 1. These variables were selected due to their importance in answering the research questions. This additional data reduction involved watching the video and coding each variable per the operational definition and value. Many of the new variables were coded with respect to the "the last glance", which is operationally defined in Section 2.2.2. Table 1 displays each variable's operational definition and counts for the existing and new variable reduction (i.e., not included in prior SHRP 2 reduction). Note the counts reflect 286 rear-end events as a filtering process (described in Section 2.3) eliminated 69 events.

2.2. Calculation of inverse time to collision (TTC^{-1}) and visual cue onset point (VCOP)

SHRP 2 data includes kinematic variables, including speed, acceleration, gyroscope, and radar. The radar data identifies the location and relative speed of up to eight objects simultaneously in the forward direction. We denote x^i_{pos} and y^i_{pos} as the position of the i^{th} object (in the current study, this was always another vehicle) relative to the instrumented vehicle. Here, x^i_{pos} was in the longitudinal position of the vehicle and y^i_{pos} was the lateral position of the vehicle with right side being positive. Please note that these distances refer to the bumper to bumper

distance, the distance between the front bumper of the ego vehicle and rear bumper of the lead vehicle (SAE International, 2015). The relative speeds in the longitudinal (x) and lateral (y) directions are denoted by $\dot{x}^i_{pos}$ and $\dot{y}^i_{pos}$ respectively.

The raw radar data were noisy. Apart from temporal noise in the speed and position values, it often failed to identify continuity of a target after an instance of occlusion. Sometimes the radar reported identification of an object when there was no object present ("ghost objects"). Therefore, the raw radar data were passed through a post processing algorithm (Gorman et al., 2015) that eliminated ghost objects, as well as used smoothing filters to eliminate noise. The output also specified if a certain object was the lead vehicle relative to the instrumented vehicle. This filtering eliminated an additional 69 events due to poor radar data, resulting in 286 rear-end events included in the analysis (278 near-crashes and 8 crashes).

2.2.1. TTC, TTC^{-1}, and looming

Time to collision (TTC) is often used to quantify proximity to a potential crash, computed as follows (Östlund et al., 2006; SAE International., 2015):

$$TTC = x^i_{pos} \Big/ \dot{x}^i_{pos} \tag{1}$$

where, TTC is the instantaneous measurement where relative speed is maintained at $\dot{x}^i_{pos}$. Similarly, inverse TTC is computed as:

$$TTC^{-1} = \dot{x}^i_{pos} \Big/ x^i_{pos} \tag{2}$$

A higher value of TTC^{-1} indicates a closer proximity to a potential crash. Close approximations of TTC and TTC^{-1} are readily available to the human visual system via the optical expansion, or *looming*, of the lead vehicle on the retina (Lee, 1976), and they have been previously implicated in driver near-crash maneuvering (e.g., Kondoh et al., 2014; Markkula et al., 2016, 2018).

2.2.2. Visual cue on point (VCOP) and last glance

The VCOP denotes the time instance when it is believed the driver received the first visual input of a potential crash. In this paper, we specified VCOP as conditional to the criticality of the event. Here, VCOP was defined based on the time instance, T_{th} where TTC^{-1} crossed a certain threshold TTC^{-1}_{th}. Formally VCOP was represented as:

$$VCOP = \begin{cases} T_{th}, & driver\ glance = forward \\ T_{th} + \Delta T, & driver\ glance \neq forward \end{cases} \tag{3}$$

Here, ΔT denoted the time duration between the TTC^{-1} value crossed TTC^{-1}_{th}, and the driver's glance returned forward (T_{LG}). This instance was also referred to as the time the "last glance" ended.

In this paper we have used two different thresholds, for C^{-1}, 0.1 and 0.2. Recent literature analyzing naturalistic crash and near crashes found that most reactions occur at an TTC^{-1} of 0.2 (Markkula et al., 2016; Victor et al., 2015;). Many researchers have argued that driver behavior, especially gaze concentration at inverse TTC value as low as 0.1 has a significant impact on the outcome of the event (e.g. Victor et al., 2015; Bärgman et al., 2015, 2017).While other studies have explored higher TTC^{-1} thresholds (Kiefer et al., 2005; Moon and Yi, 2008; Kondoh et al., 2014), this document links between driver reactions and TTC^{-1} of value 0.1 and 0.2. As this paper mostly concerns in predicting driver reactions ahead of the actual maneuver, we focus on these values.

A pictorial depiction of the VCOP, and last glance is shown in Fig. 1 for two distinct scenarios. Fig. 1 shows the value of the TTC^{-1} and the driver glance location with respect to time. In Fig. 1(a), the driver looked forward when TTC^{-1} reached C^{-1}_{th}. We denoted this time instance as the VCOP (or eyes-on-threat). However, if TTC^{-1} reached TTC^{-1}_{th} when the driver was looking away, as shown in Fig. 1(b), VCOP was defined for the time instance (T_{LG}) when the driver returned his/her gaze toward the forward roadway (or eyes-off-threat).

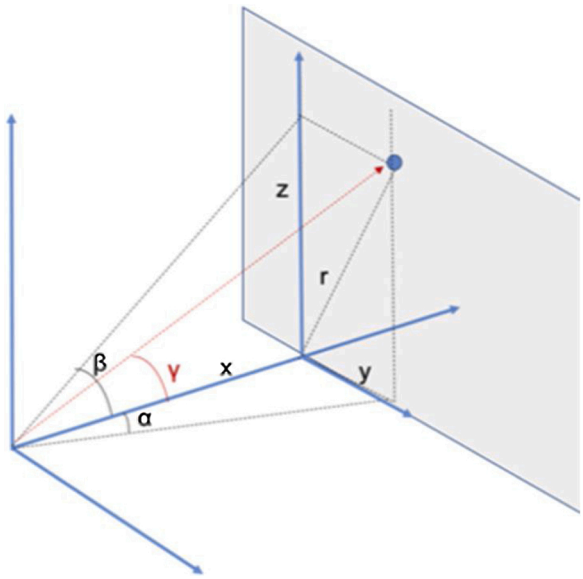

Fig. 2. Schematic for the combined gaze eccentricity or computed from the horizontal gaze eccentricity and vertical gaze eccentricity.

In this study, we captured gaze eccentricity of the driver's last glance before the safety-critical condition. A last glance was defined as the glance location away from forward roadway observed before the vehicle enters a safety-critical condition. The last glance was performed before either the subject physical reaction, or, if no subject reaction was visible, before the first significant approach of the lead vehicle becomes visible in the front facing video (i.e. looming). This specifically excluded all glances performed as a reaction to the conflict (i.e. searching for an escape path). Again, the time instance, T_{th} where TTC^{-1} crossed a certain threshold TTC^{-1}_{th} was used as a reference to identify the driver's last glance. If the driver looked forward at T_{th}, as shown in Fig. 1(a), then the last glance location prior to this was considered the last glance (if the last glance is within 10 s of T_{th}). If the driver did not look away, or there was no glance away from the forward roadway within 10 s of T_{th}, no last glance location was recorded. If the driver looked away at T_{th}, as shown in Fig. 1(b), we considered the glance location at T_{th} as the last glance. Any glance other than the last glance during this time period $t \in [T_{th} - 10\ ,\ T_{th})$ was considered eyes-off-threat. In both cases shown in Fig. 1, the TTC^{-1} threshold was considered, $TTC^{-1}_{th} = 0.1$. The VCOP computation resulted in 160 eyes-on-threat events (4 crashes and 154 near-crashes) and 126 eyes-off-threat events (4 crashes and 122 near-crashes). Eyes-on-threat cases also included the variable 'eyes on threat before VCOP' (or EOTB-VCOP), which measured the duration of forward glance between last glance and VCOP points. The EOTB-VCOP should assess the impact of the last glance on the driver's maneuver decision. If the EOTB-VCOP value was high, which meant the driver was looking forward for a long period of time before the event criticality became high, then the last glance and its associated variables (explained later in the paper) could be expected to have a limited effect on the decision of the driver.

2.3. Driver reaction and maneuver

In this analysis, two types of avoidance maneuvers were considered: *braking-only (BR)* and *Steering and Braking (SB)*. In a BR scenario, the driver decided to stay in the same lane of the conflicting lead vehicle and the maneuver was restricted only to longitudinal direction. In SB scenarios, the driver decided to steer to a different lane than the conflicting

Table 2
Variable Name, Operational Definition, and Reponses Choices for the New Variable Reduction.

Variable Name		Description	Values
Gaze Eccentricity (for last glance)	Horizontal Eccentricity	Zero vertical and horizontal glance eccentricity would be a driver looking straight ahead. Eccentricity was categorized into bins of 20 degrees (e.g., 'down between 70−90 degrees'). Then, horizontal and vertical glance events were combined and differentiated between the directions of the glances by means of the instrumented vehicle driver left/right and up/down, respectively. The middle value in the range was used in the analysis (e.g., 'down 40%' was used instead of 'down between 30−50 degrees').	'left 100 degrees' ($n = 8$), 'left 70 degrees' ($n = 4$), 'left 60 degrees' ($n = 5$), 'left 40 degrees' ($n = 18$), 'left 20 degrees' ($n = 18$), 'straight ahead' ($n = 133$), 'right 90 degrees' ($n = 5$), 'right 80 degrees' ($n = 5$), 'right 60 degrees' ($n = 13$), 'right 40 degrees' ($n = 21$), 'right 20 degrees' ($n = 55$).
	Vertical Eccentricity		'down 80 degrees' ($n = 2$), 'down 60 degrees' ($n = 23$), 'down 40 degrees' ($n = 46$), 'down 20 degrees' ($n = 16$), 'straight ahead' ($n = 168$), 'up more than 90 degrees' ($n = 0$), 'up 80 degrees' ($n = 1$), 'up 60 degrees' ($n = 1$), 'up 40 degrees' ($n = 4$), 'up 20 degrees' ($n = 25$)
Road Attention Allocation	Forward	The attention allocated to the roadway in respect to the subject's own lane, adjacent lanes, the rear of the vehicle, and the awareness of potential hazards in the present traffic environment	'full' ($n = 169$) or 'intermittent' ($n = 117$)
	Right		'yes' ($n = 44$) or 'no' ($n = 242$)
	Left		'yes' ($n = 73$) or 'no' ($n = 213$)
	Back		'yes' ($n = 56$) or 'no' ($n = 230$)
Escape Path Feasible		The feasible escape directions for an emergency maneuver. Reduced into a binary variable on the feasibility of an escape path.	'yes' ($n = 180$) or 'none' ($n = 106$)
Escape Glance		The direction of the escape glance made by the subject driver after becoming aware of an impending near crash or crash. Reduced to a binary variable of 'yes' or 'no'	'yes' ($n = 132$) or 'none' ($n = 154$)
Last Glance Location		The last glance is operationally defined in Section 2.3.2. The last glance location uses the driver glance data to define the driver's glance location during the last glance. This was reduced into a binary value of 'interior" and 'exterior'	'exterior ($n = 199$) or 'interior' ($n = 87$)
Driver Impairments		The driver intoxicated, drugged, and/or sleepy/asleep	'yes' ($n = 10$) or "no" ($n = 276$)
Secondary Task		The driver performing a secondary task	'yes' ($n = 190$) or 'no' ($n = 96$)
Maneuver		What maneuver decision the driver used	Braking ($n = 255$) or Steering ($n = 31$)

lead vehicle. In this work, we have annotated the time instance when the driver initiated the steering maneuver using the steering wheel.

2.4. Driver gaze eccentricity

We quantified the driver's gaze away from forward roadway using their horizontal and vertical deviation, termed here as *Horizontal Gaze Eccentricity* (α) and *Vertical Gaze Eccentricity* (β). As mentioned in Sec 2.1.2, in each event the driver's last glance behavior was annotated in terms of α and β, sometimes with a large range (e.g., 'down between 30–50 degrees'). In order to quantify distraction, we considered a middle value (e.g., 40 degrees for case noted as 'down between 30–50 degrees'). Now, in order to understand the combined effect of α and β, we introduced a single measure that merged the horizontal and vertical eccentricity, *Combined Gaze Eccentricity* (γ). Fig. 2 shows an illustration of this idea. Using simple geometry, γ is calculated as:

$$\gamma = \tan^{-1}\left(\sqrt{\tan^2\alpha + \tan^2\beta}\right) \tag{4}$$

2.5. Computed feature variables

In addition to the data variables obtained from the data reduction procedure, described in Table 2, we computed five new variables from the event analysis using VCOP and TTC^{-1} plot shown in Figs. 3–5; see Table 2.

2.6. Illustrative example events

Figs. 3–5 show three representative near-crash cases. These figures highlight the VCOP, physical reaction point, braking maneuver start point, steering maneuver start point, if any and the driver gaze forward. They also show the progression of TTC^{-1} over time and the TTC_{th}^{-1} value of 0.1. In events where two lead vehicles were involved, trajectory of the conflicting vehicle and the non-conflicting vehicle are shown.

Fig. 3 shows the simplest case of a BR-only event with one lead vehicle. Here the TTC^{-1} threshold was crossed when the driver's eyes were off road. The criticality of the event increased once the driver looked back at the road at the VCOP, with the driver applying brakes within one second. As a result, the TTC^{-1} drops back below the criticality level.

Fig. 4 shows an example of an SB event. Here the TTC^{-1} threshold was crossed when the driver's eyes were on road. In this specific case, two lead vehicles were involved. The host vehicle was following a vehicle (non-conflicting) until the conflicting vehicle appears to the driver's view at time $t = 459.5$. In this case, the non-conflicting vehicle changed its lane, possibly to avoid the impending threat from the conflicting vehicle. After the VCOP point, the driver immediately acknowledged the threat (physical reaction) and made evasive actions, braking and using a steering maneuver to change lanes.

Fig. 5 shows a BR event with two lead vehicles [LD1 (non-conflicting) and LD2 (conflicting)]. The instrumented vehicle was following a lead vehicle (non-conflicting) at time $t = 1491$. Then, LD1 suddenly changed lanes and another vehicle became the lead vehicle. The video shows LD1 changing lanes to avoid a collision with a slower moving LD2. As LD1 changed lanes, revealing the conflicting situation of LD2 to the instrumented vehicle driver, the situation escalated until the driver applied the brakes at $t = 1493$. The driver was looking away when the TTC^{-1} crossed the threshold.

The three cases above show that critical events, such as a near-crash, the TTC^{-1} value increases exponentially until an evasive action is taken.

3. Analysis approach

3.1. Driver reaction classification

We used two different models to predict driver maneuver (1) linear model using logistic regression (LR) and (2) non-linear model using random forest. Both models have been widely used in classification tasks (Murphy, 2012). An LR model builds a discriminative model that creates a linear combination of the features and then passes it through a logistic function to determine conditional class probability. With a predetermined threshold (often 0.5) applied to the computed probability value, a classification task is formed. An RF model is an ensemble of decision trees (DT), that learns a set of decision rules by creating a hierarchical graph structure (Ho, 1995; Rokach and Maimon, 2008). The graph constitutes a set of nodes. A parent node in the graph splits into child nodes, unless no more splitting is possible. The splitting action splits the data into a subset of data conditioned on a feature value. In general, the creation of child nodes in an DT increases the homogeneity

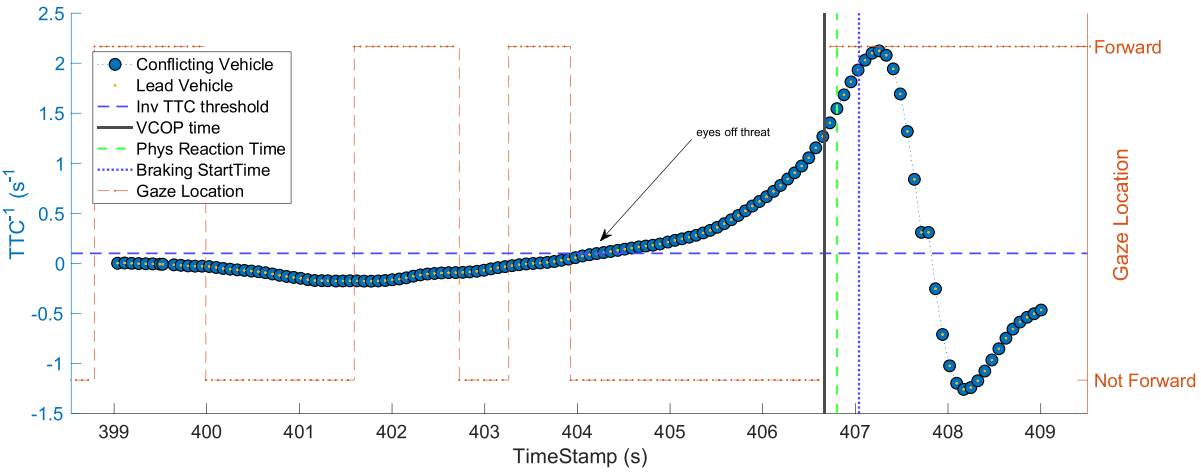

Fig. 3. Eyes-off-threat event with one lead vehicle. Here the driver applied brake as the evasive maneuver.

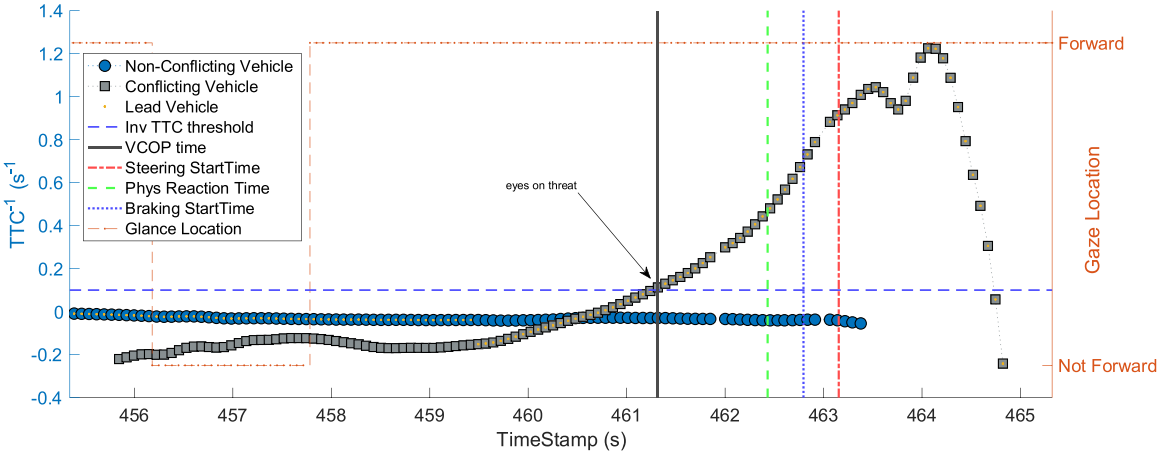

Fig. 4. Eyes-on-threat event with two lead vehicles. In this case the driver changed lane as the evasive maneuver.

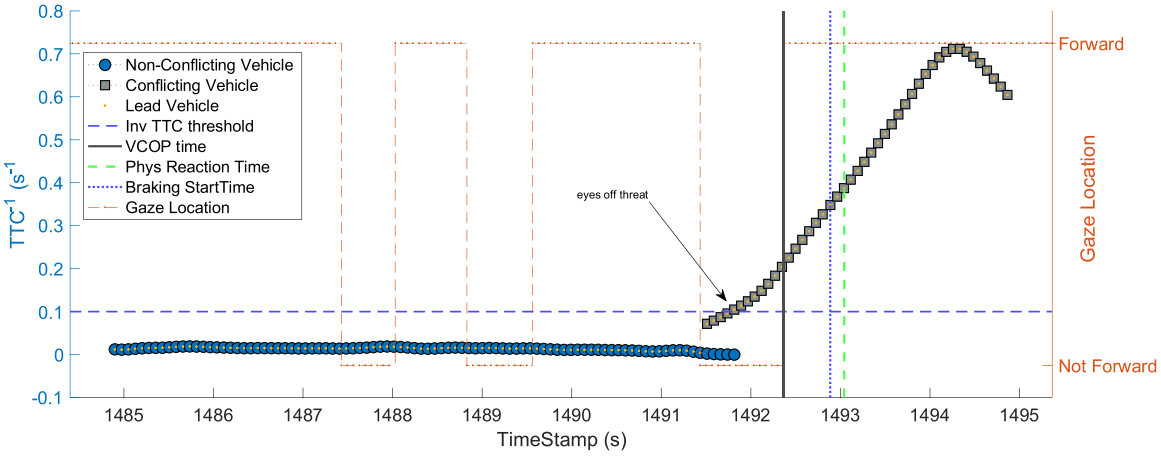

Fig. 5. Eyes-off-threat event with two lead vehicles. Here the driver applied brake as the evasive maneuver.

of the resultant nodes. RF has been successful in transportation and human factors research due to its capability in capturing nonlinear relations (Harb et al., 2009; McDonald et al., 2014, 2019a, b). One advantage of using a DT-based method is the resulting classifier is relatively interpretable, for example using standardized methods for measuring the relative importance of the feature variables.

3.1.1. *Data preprocessing*

This step mainly involves two tasks, addressing class imbalance and partitioning the full dataset into training and testing datasets. Seventy percent (70 %) of the data were used in training with the remaining thirty percent (30 %) for testing. Now, the dataset in consideration contains lesser number of events from SB maneuver compared to BR. It is known that unbalanced data can undermines the decision tree training

Table 3
Computed Variables from the VCOP Features.

Variables	Definition
VCOP Condition	Depending on the definition in Section 2.2.2 the VCOP condition has two values: 'eyes on threat', 'eyes off threat'
Last Glance Duration	Based on the glance location coded in the reduction data and definition of last glance from Section 2.2.2, last glance duration is computed as the time duration in second.
TTC at VCOP	Once VCOP point is defined, the TTC value is computed from the radar data at the VCOP timestamp.
TTC at Physical Reaction	Denotes the TTC value at the time instance of physical reaction
Last Glance Eccentricity Combined	The combined eccentricity defined by Eq. (4)
Eyes on Threat before VCOP' (EOTB-VCOP)	Computed from the glance location coded in the reduced data along with the definition of last glance and VCOP from Section 2.2.2.

process (He and Garcia, 2008). One of the standard method to address this issue is to oversample the minority class. Such over-sampling has been shown in simulation to provide more robust results than alternative methods (Pulgar et al., 2017). Therefore, we used *random oversampling* method to up-sample the SB events in order to balance the data in both BR and SB events in the training dataset. After over-sampling, the dataset contained 249 BR events and 232 SB events (originally, 29 SB events[1]). All the variables in Tables 2 and 3 were used as dependent variables in the RF model with no specific restrictions in the tree structure. As the *TTC* and TTC^{-1} are reciprocal and RF is a nonlinear method, we considered only one value. However, after checking different combinations, it appears using TTC values produced the best classification results.

3.1.2. Model training and evaluation process

The LR model and the RF model were trained in Python using the scikit-learn library (Pedregosa et al., 2011). For both the models, 70 % of the data were used for training and cross validation, the rest of the data (30 %) were used for testing. In the RF model, we used entropy as the measure for splitting the nodes. Hyperparameters were optimized using an internal cross-validation process. First, we tested the variation of the area under the curve value by varying individual parameters to assess how and when the RF overfit. After reviewing these results to better understand the data, we used three-fold cross validation with random search over the combined grid of the parameter space. The parameters used for the cross validation were (a) depth of tree, (b) number of trees in the forest (c) minimum number of samples required to initiate the split of a node, (d) maximum number of features considered at the node split, and (e) minimum samples at the split of a node. The final hyperparameters selected were 500 trees, at a depth of six in the RF model. Following the training, the models were evaluated by their accuracy, precision, and recall on the testing dataset. RF models were initially trained for of 0.1 and 0.2.

3.1.3. Model inference

Following the model training process, inference was performed using the variable importance plots from the random forest and partial dependence plots. Variable importance is a measure of the loss in accuracy associated with the iterative removal of a feature from the algorithm (James et al., 2017). This iterative calculation is limited as it does not control for contributions from other features or correlations between features. Partial dependence measures address this gap by explicitly marginalizing over all other features and calculating the impact of a feature value on classification over the range of values in the training data set (Friedman, 2001). Partial dependence is calculated using the following equations:

$$\widetilde{f}(x) = \frac{1}{n}\sum_{i=1}^{n} f(x, x_{iC}) \tag{5}$$

Where $f(x)$ was the partial dependence of feature x, n was the number of samples in the dataset, X_{iC} was the other features in the dataset, the sum was the predicted class and $f(x)$ is:

$$f(x) = \log p_k(x) - \frac{1}{K}\sum_{j=1}^{K} \log p_j(x) \tag{6}$$

Where K was the number of classes (2 in this case), k was the reference class (breaking), and p_j was the proportion of votes for the class j predicted by the random forest algorithm (Liaw and Wiener, 2002). Thus, partial dependence illustrates how changes in the value of a feature influence the predicted class (Zhao and Hastie, 2019). A final method to perform inference was to analyze the structure of the DTs from the RF. By visualizing these trees, one can see the logic chains that led to classification and the learned logical connections between variables. In this work, we visualized a single tree, the DT, with the maximum F1 score among all of the trees in the RF.

Table 4
Comparison of classification accuracy of two RF models.

	Accuracy	Precision	Recall
RF model with $TTC_{th}^{-1} = 0.1$	95.86 %	100 %	91.42 %
RF model with $TTC_{th}^{-1} = 0.2$	85.45 %	78.95 %	90.81 %
LR model with $TTC_{th}^{-1} = 0.1$	58.62 %	57.58 %	54.29 %
LR model with $TTC_{th}^{-1} = 0.2$	61.49 %	57.14 %	69.57 %

4. Results

Table 4 shows the result of the prediction for the test set of the dataset. We trained the LR model and RF models using two different inverse TTC threshold values (TTC_{th}^{-1}), 0.1 and 0.2. For $C_{th}^{-1} = 0.1$, the trained model achieved the best performance with an accuracy of 95.86 %, precision of 100 %, and recall of 91.42 % with 500 trees. As shown in Table 4, the LR model underperformed the RF model. Here and below in this paper, all accuracy/precision/recall percentages are for the performance on the test set (i.e., the 30 % of the data that were withheld during RF training). The result with $C_{th}^{-1} = 0.1$, as shown in Table 4, is better than $TTC_{th}^{-1} = 0.2$. These results suggest the RF classifier was capable of accurately predicting the drivers' maneuver and reflects the underlying reasoning. The RF model with $TTC_{th}^{-1} = 0.1$ was more accurate; thus, all the subsequent discussion is focused on models built with this threshold value.

4.1. Inference of the decision logic

In order to understand the underlying decision logic of the RF, we look deeper into the model. First, we study the relative importance of the features in the process of the decision making. Next, we a single tree from the random forest to understand a typical decision logic. This step helps us to visualize how the algorithm may be forming the decision logic. Finally, we study the partial dependence plot that shows the marginalized effect of a single variable in creating the final decision. This step helps us to identify key threshold of each of the participating variables and draw key conclusion about the decision process of a driver in a safety critical condition.

[1] One SB event was eliminated as the corresponding sensor values had noise and creating numerical instability.

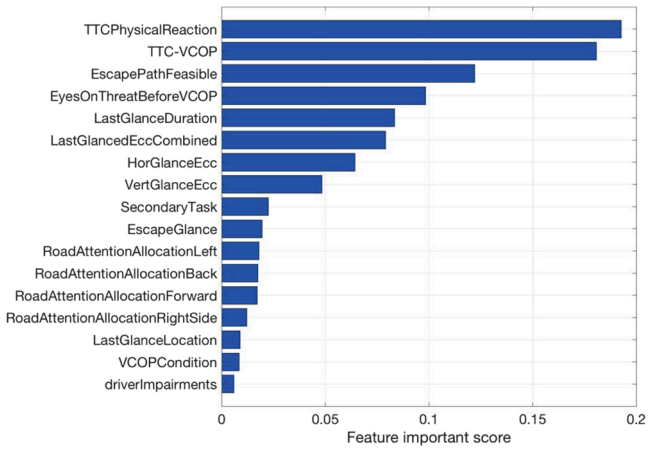

Fig. 6. Variable Importance in the RF Model.

variables compared to all feature variables, respectively. A representative structure of the DT is shown in the Fig. 7[2], where Class 1 = BR and Class 0 = SB (all had braking as the first response). The tree in Fig. 7 had the highest F1-score among all the trees. F1 score is the harmonic mean of the precision and recall.

These decision logics are possible examples the RF may use for its decision. This tree is one of the 500 trees created during the process. Every logic presented here might not be the final logic used in the final RF decision. However, these examples provide insight for the decision philosophy, which is further investigated below.

A summary of all the decision logics are shown in Table 5, where six decision paths lead to an SB output and five lead to an BR output. We summarize the DT as follows:

1 Looking deeper into decision cases 8–11 in Table 5 reveals that, when the drivers' eyes are on threat for more than about a second before the looming reaches threshold (EOTBVCOP $>$ 0.97 s), and TTC values at VCOP and physical reaction are substantially high (TTC at VCOP = 10 in these scenarios), the driver tends to make a steering maneuver if there is an escape path making the lane change feasible. They brake if the steering maneuver is not feasible. When the TTC at the physical reaction is smaller ($<=$ 4.1*s*), drivers tend to brake only, even if the steering maneuver is feasible.
2 The drivers always tend to brake only if no escape path is feasible (cases 4,5, and 6).
3 In cases when the eyes on threat time before VCOP is substantially small (*EOTBVCOP* $<$ 1.0 *second*), the driver can still choose the steering maneuver option, especially when the last glance gaze eccentricity is very high, and the lane change is feasible.

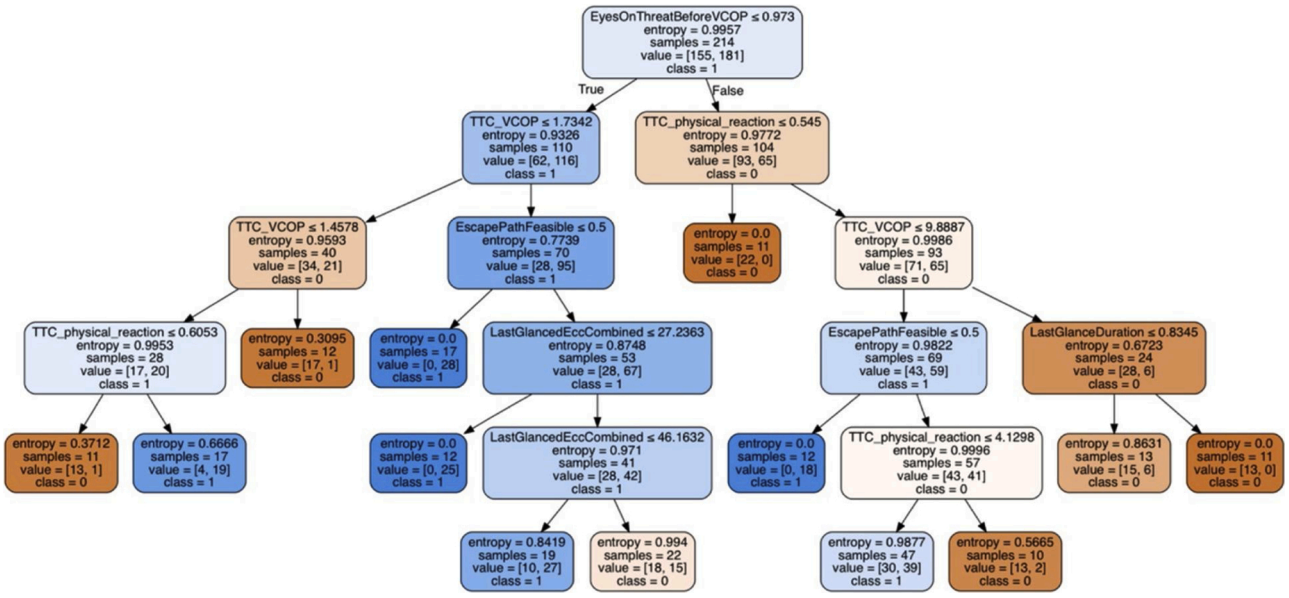

Fig. 7. Structure of a Single Decision Tree. Class = 1 represents BR and Class = 0 represents SB.

4.1.1. *Variable importance*

Fig. 6 displays the results for the analysis of the variable importance, including all the variables provided as input features to the DT. The six most important variables for classification were TTC at the Physical Reaction (19.3 % accuracy loss when removed), TTC at the VCOP (18.1 %), Escape Path Feasibility (12.2 %), EOTB-VCOP (9.8 %), Last Glance Duration (8.4 %), and Combined Last Glance Eccentricity (7.9 %). Notably, the Combined Gaze Eccentricity had higher importance than either Horizontal Eccentricity or Vertical Eccentricity. It is further notable that Secondary Task Involvement had low influence on the drivers' maneuvering decision and that drivers' maneuver decision was not dependent on Last Glance Location (outside vs inside).

4.1.2. *Random tree decision structure*

In order to understand the underlying decision logic, we used the top six predictive features shown in Fig. 6 and trained another RF. The overall performance of the RF decreased to 83 % from 96 %, using the six

4.1.3. *Partial dependence plots*

Fig. 8 displays the partial dependence plot for the six most important variables in the RF model in Fig. 6. Positive values on the y-axis indicate the driver was more likely to brake at that value of the feature, whereas negative values indicate the driver was more likely to steer and brake.

[2] The color 'blue' highlights the class = 1 cases. The color 'orange' highlights class = 0. The brightness depends on the entropy value. Higher entropy (~1) has higher brightness and lower entropy (~0) has darker shade

Table 5
Elaboration of the Decision Logic.

Decision Case	Conditions	Decision Class
Case 1	*EOTBVCOP* <= 0.973 and *TTC_VCOP* <= 1.4578 and *TTC_PhysReaction* <= 0.6053	SB
Case 2	*EOTBVCOP* <= 0.973 and *TTC_VCOP* > 1.4578 and *TTC_VCOP* <= 1.7342	SB
Case 3	*EOTBVCOP* <= 0.973 and *TTC_VCOP* <= 1.4578 and *TTC_physReaction* > 0.6053	BR
Case 4	*EOTBVCOP* <= 0.973 and *TTC_VCOP* > 1.7342 and *EscapePathFeasible* = *False*	BR
Case 5	*EOTBVCOP* <= 0.973 and *TTC_VCOP* > 1.7342 and *EscapePathFeasible* = *True* and *LastGlancedEccCombined* <= 46.1632	BR
Case 6	*EOTBVCOP* <= 0.973 and *TTC_VCOP* > 1.7342 and *EscapePathFeasible* = *True* and *LastGlancedEccCombined* > 46.1632	SB
Case 7	*EOTBVCOP* > 0.973and *TTC_PhysReaction* <= 0.545	SB
Case 8	*EOTBVCOP* > 0.973 and *TTC_PhysReaction* > 0.545 and *TTC_VCOP* > 9.8887	SB
Case 9	*EOTBVCOP* > 0.973 and *TTC_PhysReaction* > 0.545 and *TTC_VCOP* <= 9.8887 and *EscapePathFeasible* = *False*	BR
Case 10	*EOTBVCOP* > 0.973 and *TTC_PhysReaction* > 4.1298 and *TTC_VCOP* <= 9.8887 and *EscapePathFeasible* = *True*	SB
Case 11	*EOTBVCOP* > 0.973 and *TTC_PhysReaction* > 0.545 and *TTC_PhysReaction* <= 4.1298 and *TTC_VCOP* <= 9.8887 and *EscapePathFeasible* = *True*	BR

Values near zero indicate that the feature does not significantly contribute to classification at that value. The gray bars are a rug plot that shows the distribution of the feature values in the dataset. The plots show two straightforward trends: (1) when an escape path was not feasible, the driver was likely to brake; and (2) when the last glance duration was above 1.3 s, the driver was more likely to brake. The trends of variables TTC at VCOP, TTC and Physical Reaction, and Combined Gaze Eccentricity are more difficult to interpret. The plots show that braking is more likely in the range between 1.5 s and 8.5 s TTC at VCOP. TTC at the Physical Reaction less than zero indicates that steering is more likely (a negative TTC value indicates the relative distance between the vehicles was increasing), however, this trend is biased by the relatively few samples less than zero and should be investigated further in future work. Combined Gaze Eccentricities less than 9 degrees led to substantially increased likelihood of braking; however, Combined Gaze Eccentricities greater than 100 degrees did not have a strong effect.

Two-dimensional partial dependence plots which show algorithm predictions across two variables provide additional insight into the algorithm predictions. Two examples of these plots are shown in Figs. 9 and 10. Fig. 9 shows the two-dimensional partial dependence plot for TTC at the Physical Reaction and Escape Path. In the figure, black squares indicate the highest likelihood in predicting a lane change maneuver and the white squares indicate the highest likelihood in predicting braking. The figure shows that when there is no escape path, the TTC at the Physical Reaction has little impact on the model's predictions, however, when there is a feasible escape path, drivers are more likely to brake at very low and high values of TTC at the Physical Reaction.

Fig. 10 shows the two-dimensional partial dependence plot for last glance eccentricity combined and last glance duration. Changes in these variables primarily increased the likelihood of the algorithm in predicting braking (lighter squares in this case indicate no effect on predictions). The highest likelihood of braking prediction occurred when last glance duration and gaze eccentricity were 0 (i.e., the driver was looking straight ahead). Braking predictions were more likely across the spectrum of duration when the gaze eccentricity was less than 50; however, as eccentricity increased beyond 50, gaze duration and gaze eccentricity were less likely to predict braking. Generally, this figure illustrates a lack of interaction between glance eccentricity and duration.

5. Discussion

In this analysis we investigated drivers' maneuver decisions during real-world rear-end crashes and near-crashes, extending prior research in this domain by including specific gaze eccentricity measures and visual looming-relative features—via the visual cue onset point. The analysis here suggests that these gaze parameters, scenario kinematics, and the driving environment (e.g., escape path feasibility) are sufficient to predict driver braking or steering and braking responses with high accuracy. Further the variable importance results show that the TTC at the driver's physical reaction, the TTC at the visual cue onset point, the presence of an escape path, the last time that the driver's eyes were on the threat before the visual cue onset point, and the last glance eccentricity and duration are the most important features for predicting driver evasive maneuver choices. The partial dependence and decision tree analysis further highlight the ranges of these features that lead to maneuver choices.

The overall predictive accuracy of the RF model compares favorably to prior machine learning based evasive maneuver prediction algorithms. For example, Hu et al. (2017) found 80.3 % accuracy differentiating between braking and lane change maneuvers and Harb et al. (2009) found 76 % accuracy identifying maneuvers in rear-end collisions. Although it is difficult to directly compare these results to the 95 % accuracy observed in this analysis due to the differences in features, datasets, and training processes, the results suggest that random forests trained with the features used in this analysis are a promising method for prediction driver maneuver decisions. These findings should be further validated with additional data; however, after validation RFs, such as the one trained here, may be used in driver process models to accurately represent driver decision making.

The inferential analysis here also agrees with prior work. Harb et al. (2009) and Kaplan and Prato (2012) found that roadway features such as the number of lanes were important for driver avoidance maneuver decision making. Although we did not explicitly model roadway type our findings that the availability of an escape path was an important feature in classification, and that when escape paths were feasible it was likely that drivers steered and braked agree with both studies. These findings also align with the model proposed in Markkula et al. (2018) which suggests that steering avoidance is subject to the availability of evidence to the driver that it is safe to change lanes. Our findings add to these earlier works in that they more clearly describe the relationship between escape paths, maneuvers, and scenario kinematics. Availability of an escape path predicted a steering except in cases when the driver's awareness of the imminent threat (TTC at Physical Reaction) occurred when the instrumented vehicle was close to the lead vehicle (*TTC at Physical Reaction* <= 4.1*s*). This suggests a crash was imminent and the time to perform a steering maneuver would be insufficient to

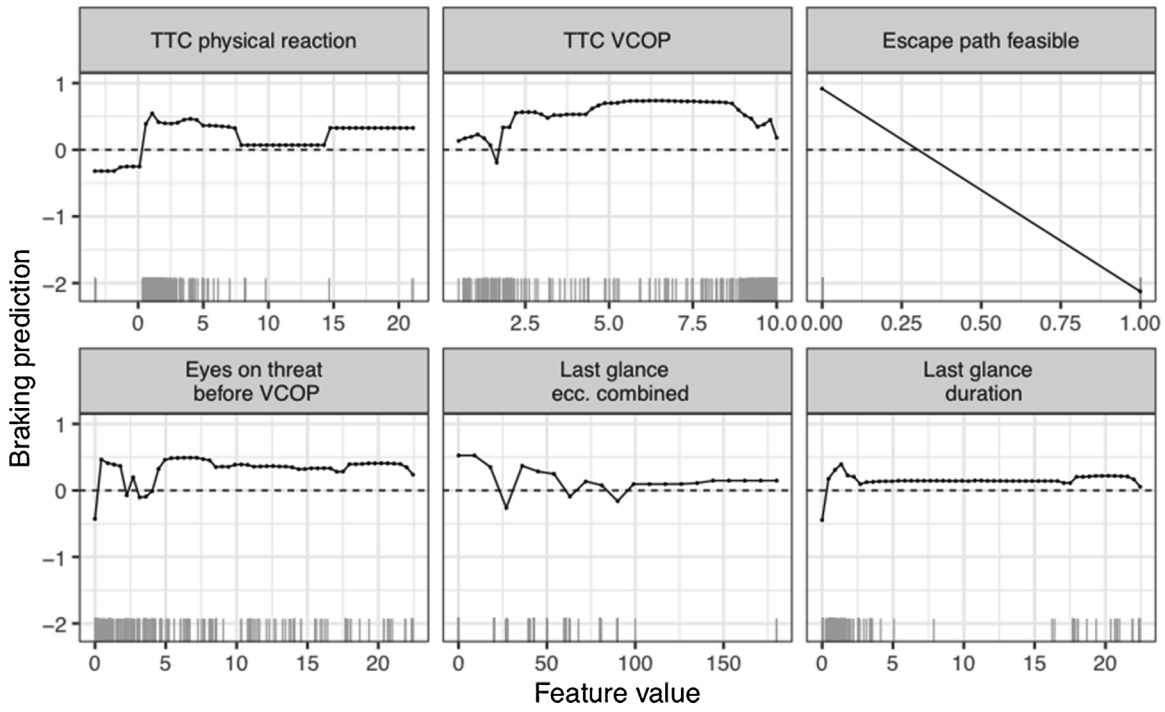

Fig. 8. Partial dependence plot for six most important variables.

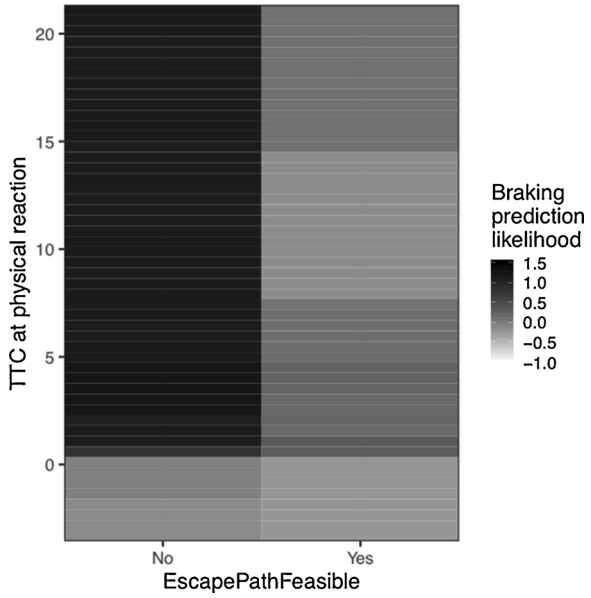

Fig. 9. Two-dimensional partial dependence plot showing the interaction between the TTC at physical reaction and Escape path feasibility. The color scale indicates the likelihood that the algorithm predicted braking, where darker squares indicate higher likelihood of braking.

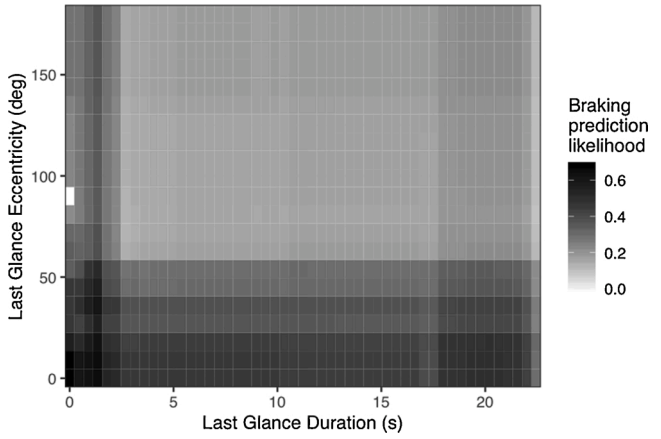

Fig. 10. Two-dimensional partial dependence plot for Last glance gaze eccentricity and last glance duration.

avoid the crash (i.e., late detection); thus, making braking only more likely.

The importance of visual kinematic evidence in our model agrees with the findings of the models discussed in Venkatraman et al. (2016); Hu et al. (2017); Xue et al. (2018), and Markkula et al. (2016). Our model is influenced primarily by two types of kinematic information: the TTC at physical reaction and the TTC at the visual cue onset point. These points reflect the driver's acknowledgment of the scenario criticality and the likely first available visual evidence of the emergency scenario, respectively. In general, the importance of these variables adds to the mounting evidence of the importance of perceived kinematics in driver decision making and behavior (Markkula et al., 2016, 2018). More specifically, our thresholds show that steering is more likely for TTC values at the physical reaction near zero and less than zero. Video review of these cases showed that TTC values less than zero represent cases where drivers initially braked then realized that a lane change would be safe and executed it. This behavior supports the evidence accumulation framework established in the Markkula et al. (2018) model.

The inclusion of quantitative last glance gaze eccentricity and duration metrics are novel additions in this analysis compared to prior work on driver decision making models. The results suggest that both eccentricity and duration are important for driver evasive maneuver decision making. However, the contribution of these variables is complex as illustrated in Figs. 8 and 10. The figures suggest that gaze eccentricities less than 46.1 degrees from center are likely to lead to driver braking and that in this range the effect of eccentricity dominates the effect of duration. In larger eccentricities the current model suggests that eccentricity does not significantly contribute to classification (i.e. the

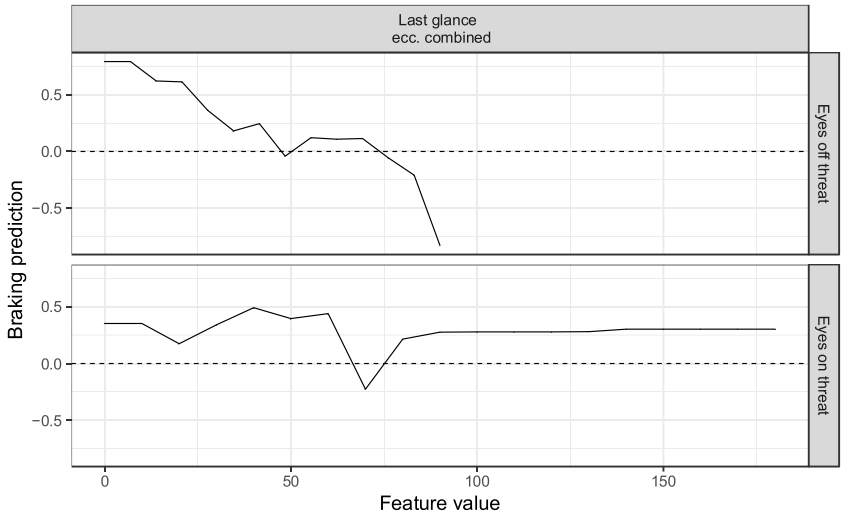

Fig. 11. Partial dependence of last glance gaze eccentricity for eyes on and eyes off threat examples.

partial dependence is near zero). This is not surprising given that there is some question regarding drivers' ability to identify hazard in the peripheral vision region of the eyes (Larson and Loschky, 2009). It is notable that the 46.1 degree threshold found in this study is well within the 90 degree detection threshold reported in Lamble et al. (1999), albeit the Lamble et al. study focused specifically on vertical eccentricity. The findings also agree with that of Huestegge and Böckler (2016) who manipulated gaze eccentricity and hazard severity in a static traffic hazard perception task (i.e., looking at traffic images on a computer screen) and found that hazard detection was the same for central and peripheral vison for dangerous hazards, but medium hazards resulted in a significant decline from central to peripheral vision. A final notable observation in the model is the role of eccentricity in eyes on threat versus eyes-off-threat CNC which is illustrated in Fig. 11. The figure shows a trend of an increased likelihood of steering and braking as gaze eccentricity increases in eyes off threat cases and a more stable trend of increased likelihood of braking in cases where the driver had their eyes on the threat. Future work should explore the former trend in more detail.

In general, longer Last Glance Durations (especially those greater than 0.8345 s) were associated with a braking response, whereas very brief Last Glance Durations were associated with a lane change maneuver. Combined with the finding that drivers' Last Glance Duration was highly correlated with TTC^{-1} at the start of the last glance ($r = 0.61$), this suggests that drivers made a decision, based on the following distance to the lead vehicle, on the length of time they could look away from the forward roadway (i.e., the criticality of the situation was low; thus, a longer glance was judged as safe) and then responded. This finding is in line with the studies by Eiríksdóttir (2016) and Victor et al. (2015) plotted the change rate in TTC^{-1} as a function of drivers' last glance duration in rear-end crashes and near-crashes in the ANNEXT and SHRP2 NDS datasets, respectively. Both found the rate of criticality in the event during the last glance was inversely related to the length of the last glance (e.g., the rate of criticality decreased as the length of the last glance increased).

5.1. Limitations

Despite these promising results, this analysis has several limitations. Due to the lack of eye tracking software, gaze eccentricity was measured using estimations from review of the video. For this reason, gaze eccentricity was measured in ranges (see Table 2) as it was deemed too unreliable to estimate specific eccentricities. Although these ranges were largely based on manual eye glance reduction, it is difficult to be certain where the driver was looking independent of the drivers' head position. Drivers' secondary task and driver impairment were reduced to binary variables, which may not reflect the variability in the intensity of specific sub-categories of secondary tasks (e.g., texting) and driver impairment (e.g., sleep) in the derived prediction algorithm. Also, there were only eight crashes included in the analysis; thus, the findings generally pertain to rear-end near crashes. Subsequent analyses should validate these findings with more granular measures of eccentricity and a larger dataset that may validate the model's predictions.

6. Conclusions

In this paper we have shown that an RF model can efficiently predict drivers' maneuver in a rear-end crash, and near crash scenario given the contextual features extracted from the event analysis and annotations. We reviewed 286 rear-end crash and near-crash events from the SHRP2 data and manually coded behavioral features. This paper specifically focused on the visual perception of drivers during rear-end events and the corresponding physical reaction and related them to the event criticality using features like TTC. We also assessed the effect of drivers' gaze eccentricity and total time spent for evidence accumulation through VCOP and EOTB-VCOP. To the best of our knowledge, this is the first effort that evaluated drivers' maneuver responses using large- scale naturalistic rear-end crash and near-crash events to understand the combined significance of driver attention, driver perception, and driver reaction. The study explores the relative importance and nonlinear pattern of interactions between these behavioral and situational variables. As a result, we have developed a RF-based algorithm that can efficiently predict the drivers' maneuver in with high accuracy. The RF explores the nonlinear pattern of interactions between the behavioral and situational variables. We have quantitatively shown the relative importance of each contributing factor in the drivers' decision making, our main conclusions are:

1 The first driver response in rear-end crashes and near-crashes are predominantly applying the brake (slowing down).
2 The feature importance analysis showed that Last Glance Duration, Last Glance Combined Gaze Eccentricity, TTC at Physical Reaction, Escape Path Feasibility, TTC at Visual Cue Onset Point, and Eyes On Threat Before Visual Cue Onset Point played vital roles in drivers' decision-making process in braking and/or changing a lane.
3 Inverse TTC threshold of 0.1 (which is equivalent to TTC value of 10 s) provides better performance compared to inverse TTC value of 0.2 (equivalently, TTC value of 5 s).

4 The feasibility of an escape path is the most prominent governing factor in the decision-making process of the driver in making a steering maneuver.
5 In general, longer last glance durations were associated with a braking maneuver and shorter last glance locations were associated with a steering maneuver. Increasing values of Combined Gaze Eccentricity up to 46.1632 degrees during the last glance increased the likelihood of a braking maneuver.

CRediT authorship contribution statement

Abhijit Sarkar: Methodology, Software, Validation, Formal analysis, Writing - original draft, Visualization, Data curation. **Jeffrey S. Hickman:** Methodology, Validation, Data curation, Writing - original draft, Funding acquisition, Visualization. **Anthony D. McDonald:** Conceptualization, Methodology, Formal analysis, Writing - original draft, Visualization, Funding acquisition. **Wenyan Huang:** Software, Formal analysis, Data curation, Visualization. **Tobias Vogelpohl:** Data curation. **Gustav Markkula:** Conceptualization, Methodology, Writing - review & editing.

Declaration of Competing Interest

This manuscript has not been submitted to, nor is under review at, another journal or other publishing venue.

The authors have no affiliation with any organization with a direct or indirect financial interest in the subject matter discussed in the manuscript.

Acknowledgements

This project was supported through a grant from the U.S. Department of Transportation (Grant No: 69A3551747115) to the Safety through Disruption (Safe-D) University Transportation Center (UTC). The SAFE-D UTC is a collaboration between the Virginia Tech Transportation Institute, Texas A&M Transportation Institute, and San Diego State University (Project# 03-036). Gustav Markkula was supported by the UK Engineering and Physical Sciences Research Council (EPSRC), grant EP/S005056/1. The authors would also like to thank Hananeh Alambeigi for her contributions to the interpretations of the partial dependence and variable importance plots. The opinions expressed in the paper are those of the authors and do not necessarily represent official positions of any government agency.

References

Bärgman, J., Lisovskaja, V., Victor, T., Flannagan, C., Dozza, M., 2015. How does glance behavior influence crash and injury risk? A 'what-if' counterfactual simulation using crashes and near-crashes from SHRP2. Transp. Res. Part F Traffic Psychol. Behav. 35, 152–169.
Bärgman, J., Boda, C.-N., Dozza, M., 2017. Counterfactual simulations applied to SHRP2 crashes: the effect of driver behavior models on safety benefit estimations of intelligent safety systems. Accid. Anal. Prev. 102, 165–180.
Dingus, T.A., Hankey, J.M., Antin, J.F., Lee, S.E., Eichelberger, L., Stulce, K.E., Perez, M., McGraw, D., Stowe, L., 2015. Naturalistic Driving Study: Technical Coordination and Quality Control. Report S2-S06-RW-1. National Academies of Science Engineering and Medicine, Washington, DC.
Dozza, M., 2013. What factors influence drivers' response time for evasive maneuvers in real traffic? Accid. Anal. Prev. 58, 299–308.
Eiríksdóttir, H., 2016. Quantitative Analysis of Rear-End Crash Causation Mechanisms Based on Naturalistic Crash Data. Masters thesis. Chalmers University of Technology, Göteborg, Sweden.
Engström, J., Werneke, J., Bärgman, J., Nguyen, N., Cook, B., 2013. Analysis of the role of inattention in road crashes based on naturalistic on-board safety monitoring data. Paper Presented at the 3rd International Conference on Driver Distraction and Inattention.
Friedman, J.H., 2001. Greedy function approximation: a gradient boosting machine. Ann. Statist. 29 (5), 1189–1232.
Gorman, T., Stowe, L., Hankey, J., 2015. S31: NDS data dissemination activities. Task 1.6: Radar Post-Processing.
Harb, R., Yan, X., Radwan, E., Su, X., 2009. Exploring precrash maneuvers using classification trees and random forests. Accid. Anal. Prev. 41 (1), 98–107.
He, H., Garcia, E.A., 2008. Learning from imbalanced data. IEEE Trans. Knowl. Data Eng. (9), 1263–1284.
Ho, T.K., 1995. Random decision forests. Paper Presented at the Proceedings of 3rd International Conference on Document Analysis and Recognition.
Hu, M., Liao, Y., Wang, W., Li, G., Cheng, B., Chen, F., 2017. Decision tree-based maneuver prediction for driver rear-end risk-avoidance behaviors in cut-in scenarios. J. Adv. Transp. 2017.
Huestegge, L., Böckler, A., 2016. Out of the corner of the driver's eye: peripheral processing of hazards in static traffic scenes. J. Vis. 16 (2), 11-11.
James, G., Witten, D., Hastie, T., Tibshirani, R., 2017. An Introdcution to Statistical Leanring with Applications in R. Springer Science+Business Media, New York.
Kaplan, S., Prato, C.G., 2012. Associating crash avoidance maneuvers with driver attributes and accident characteristics: a mixed logit model approach. Traffic Inj. Prev. 13 (3), 315–326.
Kiefer, R.J., LeBlanc, D.J., Flannagan, C.A., 2005. Developing an inverse time-to-collision crash alert timing approach based on drivers' last-second braking and steering judgments. Accid. Anal. Prev. 37 (2), 295–303.
Klauer, S.G., Dingus, T.A., Neale, V.L., Sudweeks, J.D., Ramsey, D.J., 2006. The Impact of Driver Inattention on Near-Crash/Crash Risk: an Analysis Using the 100-Car Naturalistic Driving Study Data. National Highway Traffic Safety Administration, Washington, DC.
Kondoh, T., Nobohiru, F., Hirose, T., Sawada, T., 2014. Direct evidence of the inverse of TTC hypothesis for driver's perception in car-closing situations. Int. J. Automot. Eng. 5, 121–128.
Lamble, D., Laakso, M., Summala, H., 1999. Detection thresholds in car following situations and peripheral vision: implications for positioning of visually demanding in-car displays. Ergonomics 42 (6), 807–815.
Larson, A.M., Loschky, L.C., 2009. The contributions of central versus peripheral vision to scene gist recognition. J. Vis. 9 (10), 6.
Lee, D.N., 1976. A theory of visual control of braking based on information about time-to-collision. Perception 5 (4), 437–459.
Lee, J.D., 2018. Perspectives on automotive automation and autonomy. J. Cogn. Eng. Decis. Mak. 12 (1), 53–57.
Liaw, A., Wiener, M., 2002. Classification and Regression by Random forest, 2/3. R News, pp. 18–22.
Markkula, G., Engström, J., Lodin, J., Bärgman, J., Victor, T., 2016. A farewell to brake reaction times? Kinematics-dependent brake response in naturalistic rear-end emergencies. Accid. Anal. Prev. 95, 209–226.
Markkula, G., Romano, R., Madigan, R., Fox, C.W., Giles, O.T., Merat, N., 2018. Models of human decision-making as tools for estimating and optimizing impacts of vehicle automation. Transp. Res. Rec. 2672 (37), 153–163.
McDonald, A.D., Lee, J.D., Schwarz, C., Brown, T.L., 2014. Steering in a random forest: ensemble learning for detecting drowsiness-related lane departures. Hum. Factors 56 (5), 986–998.
McDonald, A.D., Ferris, T.K., Wiener, T.A., 2019a. Classification of driver distraction: a comprehensive analysis of feature generation, machine learning, and input measures. Hum. Factors J. Hum. Factors Ergon. Soc. https://doi.org/10.1177/0018720819856454.
McDonald, A.D., Alambeigi, H., Engström, J., Markkula, G., Vogelpohl, T., Dunne, J., Yuma, N., 2019b. Toward computational simulations of behavior during automated driving takeovers: a review of the empirical and modeling literatures. Hum. Factors J. Hum. Factors Ergon. Soc. 61 (4), 642–688.
Moon, Seungwuk, Yi, Kyongsu, 2008. Human driving data-based design of a vehicle adaptive cruise control algorithm. Veh. Syst. Dyn. 46 (8), 661–690. https://doi.org/10.1080/00423110701576130.
Murphy, K.P., 2012. Machine Learning: a Probabilistic Perspective. MIT press.
Najm, W.G., Ranganathan, R., Srinivasan, G., Smith, J.D., Toma, S., Swanson, E., Burgett, A., 2013. Description of Light-Vehicle Pre-Crash Scenarios for Safety Applications Based on Vehicle-to-Vehicle Communications. National Highway Traffic Safety Administration, Washington, DC.
National Highway Traffic Administration, 2017. Traffic Safety Facts 2015. Report No. DOT HS 812 384. National Highway Traffic Administration, Washington, DC.
Östlund, J., Nilsson, L., Törnros, J., Forsman, Å., 2006. Effects of Cognitive and Visual Load in Real and Simulated Driving. Statens väg-och transportforskningsinstitut.
Pedregosa, F., Varoquaux, G., Gramfort, A., Michel, V., Thirion, B., Grisel, O., et al., 2011. Scikit-learn: machine learning in Python. J. Mach. Learn. Res. 12 (2), 825-2,830.
Pulgar, F.J., Rivera, A.J., Charte, F., del Jesus, M.J., 2017. On the impact of imbalanced data in convolutional neural networks performance. Paper Presented at the International Conference on Hybrid Artificial Intelligence Systems.
Rokach, L., Maimon, O.Z., 2008. Data Mining with Decision Trees: Theory and Applications, 2nd ed. World Scientific Publishing Co. Pte. Ltd.
SAE International, 2015. Ground Vehicle Standard: Operational Definitions of Driving Performance Measures and Statistics. J2944_201506. https://doi.org/10.4271/J2944_201506.
Senders, J.W., Kristofferson, A., Levison, W., Dietrich, C., Ward, J., 1967. The attentional demand of automobile driving. Highway Res. Rec. 195, 15–33.
Seppelt, B.D., Victor, T.W., 2016. Potential solutions to human factors challenges in road vehicle automation. Road Vehicle Autom. 3, 131–148. Springer.
Svärd, M., Markkula, G., Engström, J., Granum, F., Bärgman, J., 2017. A quantitative driver model of pre-crash brake onset and control. In: Proceedings of the Human Factors and Ergonomics Society Annual Meeting, 61, pp. 339–343. https://doi.org/10.1177/1541931213601565 (1).
Venkatraman, V., Lee, J.D., Schwarz, C.W., 2016. Steer or brake?: Modeling drivers' collision-avoidance behavior by using perceptual cues. Transp. Res. Rec. 2602 (1), 97–103.

Victor, T., Dozza, M., Bärgman, J., Boda, C.-N., Engström, J., Flannagan, C., Markkula, G., 2015. Analysis of Naturalistic Driving Study Data: Safer Glances, Driver Inattention, and Crash Risk. National Academy of Sciences, Washington, DC.

Xue, Q., Markkula, G., Yan, X., Merat, N., 2018. Using perceptual cues for brake response to a lead vehicle: comparing threshold and accumulator models of visual looming. Accid. Anal. Prev. 118, 114–124.

Zhao, Q., Hastie, T., 2019. Causal interpretations of black-box models. J. Bus. Econ. Stat. 1–19. https://doi.org/10.1080/07350015.2019.1624293.